# The effect high-dose-rate brachytherapy implant deformations have on a treatment plan and evaluation parameters

Written by: Aaron Babier

Published on March 30, 2015

# Contents

# Acknowledgements

I would like to thank Dr. Chandra Joshi for his encouragement, and patience throughout this project. His support and guidance helped make this thesis possible.

I would also like to thank Kevin Alexander and Christopher Jechel for the guidance they provided in interpreting treatment plan files.

# Acronyms

| Acronym | Definition |
|---|---|
| AAPM | American Association for Physicists in Medicine |
| ABS | American Brachytherapy Society |
| $DHI$ | Dose Homogeneity Index |
| GO | Geometrical Optimization |
| HDR-BT | High-Dose-Rate Brachytherapy |
| IPSA | Inverse Planning Simulated Annealing |

# Symbols

| Symbol | Definition |
|---|---|
| $V_{100}$ | Represents the fraction of prostate volume receiving at least 100% of the prescribed dose |
| $V_{150}$ | Represents the fraction of prostate volume receiving at least 150% of the prescribed dose |
| $U_{125}$ | Represents the total volume of the urethra receiving at least 125% of the prescribed dose, divided by 1cm$^3$ |
| $DHI$ | A measure that reflects the degree of dose uniformity for a treatment plan, defined by Equation 1.1 |

# Abstract

The objective is to determine the maximum variance in internal geometry before a treatment plan becomes invalid for high-dose-rate brachytherapy (HDR-BT). Dose delivery was modelled using a code written in MATLAB. Following a simulated catheter shift or volume deformation, the dose volume parameters were determined. When the dose volume parameters did not satisfy the guidelines imposed by the American Brachytherapy Society (ABS), the plan was deemed invalid for the associated geometric change. The maximum catheter displacement before the treatment plan became invalid was 3.70 $\pm$0.15 mm and 4.15 $\pm$0.15 mm, for inferior and superior displacements respectively. Additionally the prostate could expand 10.7 $\pm$ 0.5% or contract 11.0 $\pm$ 0.2% from its original volume before a new treatment plan would need to be determined. Typical catheter displacement was determined to have a significantly larger impact on changes in dose distribution, than average prostate volume changes. These results provide a more concrete understanding for how robust a prescribed treatment plan is to changes in geometry.

# Chapter 1

# Introduction

## 1.1 Background

Prostate cancer is the most diagnosed cancer among men in Canada, and is the third leading cause of cancer related deaths [1]. HDR-BT is a form of radiation therapy that is gaining popularity for treating prostate cancer. The treatment occurs in fractions spanning a few minutes but is typically completed over 24 hours because fractions must occur at least six hours apart [2]. To initiate HDR-BT a radiation dose will be prescribed, and then catheters will be inserted accordingly around the target site, as in Figure 1.1. Ideally the catheters will remain inside the patient throughout the course of the entire treatment.

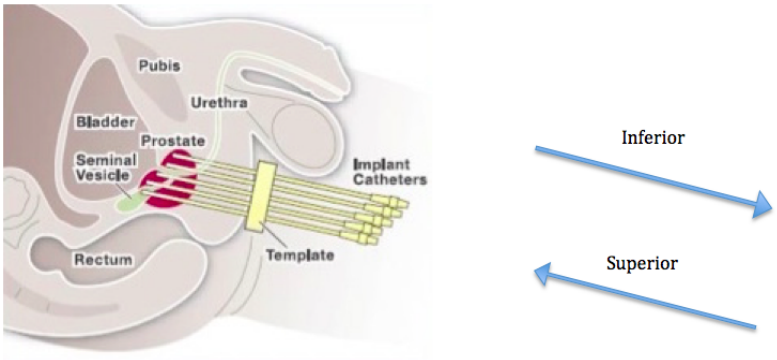


**Figure 1.1:** The catheters have injected around treatment site. The inferior and superior arrows lie along the longitudinal axis, and put the orientation of the patient into context [3].

The first fraction in the treatment should occur on the same day catheters are inserted [2]. During a fraction, a radioactive source is directed to various depths inside each catheter, as prescribed by the dwell position parameter in the treatment plan. Additionally, the time a source remains at a dwell position is indicated by the dwell time. These dwell positions and dwell times are determined in advance by a planning system and contained in a treatment plan. The parameters are chosen to produce a dose distribution that matches the prescribed dose relatively well.

The radiation dose distributions have large gradients so this treatment option is highly sensitive to catheter implant geometry. Unfortunately the prostate and surrounding region are not rigid bodies which poses a significant problem for this procedure. Catheter insertion is known to induce trauma around the target site, resulting in relatively unpredictable changes in internal geometry. Commonly the prostate will experience changes in volume and catheters will be displaced along the longitudinal axis, which causes variation in the radiation dose distribution. In the event of severe geometric changes a new dose plan may need to be created, which can also involve readjusting catheter positions.

Every treatment plan can be related to dose volume parameters, which essentially describe its effectiveness. A dose volume parameter defines the fraction of a structure volume receiving at least a specified amount of dose. Typically the dose amount is related to the dose prescribed to treat the target volume. Although brachytherapy provides relatively concentrated dose, there is no method for localizing the dose entirely to specified points. Instead the goal is to deliver the prescribed dose to at least 90% of the target volume ($V_{100} = 90\%$) [2]. Other structures that demand attention are the bladder, urethra, and rectum because of their close proximity to the prostate. The dose delivered to the bladder and rectum should not exceed 75% of the prescribed dose, in more than 1 $cm^3$ of their respective volumes [2]. In contrast it is acceptable for 125% of the prescribed dose to reach a maximum of 1 $cm^3$ of the urethra volume ($U_{125} = 100\%$) [2]. These limitations on dose volume parameters provide the backbone for determining whether or not a dose plan is acceptable.

## 1.2 Current Situation

The relevant movements that contribute to geometric changes are largely time dependent [4]. Changes in internal geometry between fractions can severely alter the projected dose distribution, so reevaluating the dose plan prior to treatment is critical. As an example, it is reasonable to expect $V_{100}$ values to decrease by 19.8% between successive fractions [5]. The most significant alterations in dose distribution are attributed to changes in catheter positions relative to the prostate [4–6]. .

Catheter displacements can be induced by several factors including organ motion, intra-abdominal pressure, and skin elasticity. Specifically these factors will eject the catheter template away from the body [7]. Since the catheters are gripped tightly within the template, the most significant movement that the catheters undergo is as a complete unit as in Figure 1.2 [7]. Between the first two fractions, the primary catheter displacement from the prostate occurs along the longitudinal axis averaging 7.6 mm [7]. However in the most extreme cases, the displacement has been cited as high as 42mm [5].

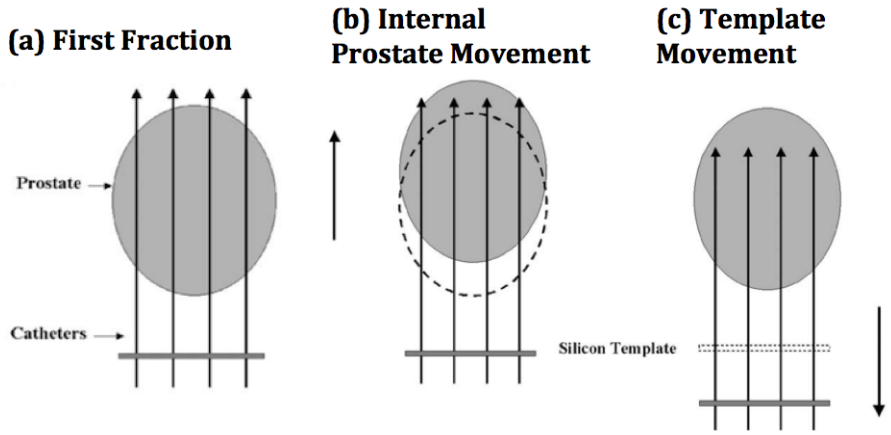


**Figure 1.2:** Potential scenarios for catheter movement relative to the prostate [5]. Scenario (a) is the catheter position before the first fraction. Scenarios (b) and (c) illustrate the most common forms of catheter movement relative to the prostate.

Most catheter movement occurs between the first two fractions and in successive fractions catheter shifts are typically less than 3 mm [7–9]. When catheters are shifted more than 3 mm from where the original treatment plan was determined, the treatment is likely to fail [10].

During treatment, the prostate volume has been observed to both decrease by as much as 13%, and increase by 17% [6].These volume changes typically occur isotropically [6]. In studies involving at least fifty patients, the average volume changes have been between 1% and 2.7% over the course of treatment [4, 9]. In extreme cases volume deformation is a major factor for changes in dose distribution. Figure 1.3 reflects the variability of dose volume parameters following volume deformations.

The primary issue with comparing clinical studies focusing on HDR-BT, is that clinical regulations are variable between studies. This means that treatment plans are optimized for different dose volume parameters. Additionally, treatment plans

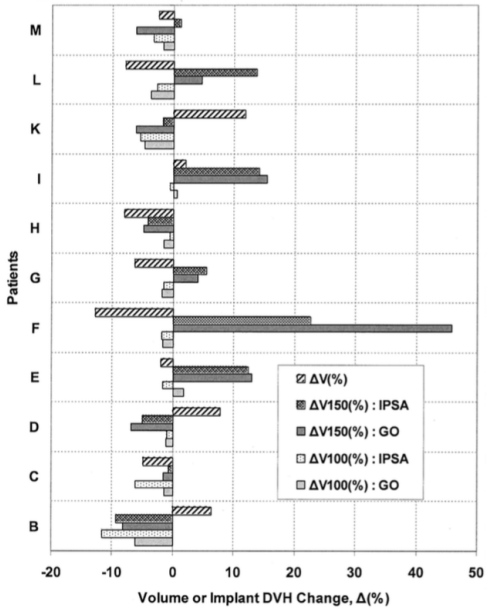


**Figure 1.3:** Between fractions for eleven different patients, the change in prostate volume, $V_{100}$, and $V_{150}$ were recorded. Two different dose optimization techniques (IPSA and GO) are also compared. Data for patient A and J was not published on the graph [6].

developed with different planning techniques will have variable levels of geometric resilience (Figure 1.3). Thus the allowed range for implant deformation will be dependent on optimization technique used to generate the treatment plan.

Different planning techniques prioritize various elements over others [11]. Two optimization algorithms for HDR-BT are geometrical optimization (GO) and inverse planning simulated annealing (IPSA). GO focuses on creating a uniform dose distribution but ignores the dose to the organs at risk [12]. In contrast, IPSA creates a dose distribution that conforms to the target tissues, and limits the dose to organs at risk [12]. IPSA is widely considered to be the superior technique because it can achieve better $DHI$ and is more efficient to implement [11, 12].

The techniques used to measure catheter displacement have also lead to variable results for average catheter displacement [9]. These techniques also tend to have high uncertainty, largely in part to the resolution associated with imaging the prostate. Uncertainty in most measurement techniques is restricted to the spacing between CT scan planes [9]. This spacing is typically similar in magnitude to average catheter displacements.

The degree to which dose uniformity changes with prostate geometry is not well established. Dose homogeneity index (DHI) provides a measure for how uniform the dose distribution is and is defined as

$$DHI = 1 - \frac{V_{150}}{V_{100}} \tag{1.1}$$

A high DHI is favourable because it implies that there are less dose hot spots in the target site. Although $DHI$ is not typically measured while treating prostate cancer with HDR-BT, it is commonly used while treating breast cancer. The ABS does not include a guidelines for $DHI$ while treating prostate cancer but for breast cancer they recommend that the $DHI$ is larger than 75% [13]. In research independent from ABS the optimal $DHI$ for treating prostate cancer with HDR-BT was found to be $0.62 \pm 0.06$ [14].

## 1.3 Motivation

A more sophisticated understanding as to how geometric changes impact a dose distribution could improve the treatment planning process. A treatment plan containing information for the extent of allowed variations in geometry, would help determine whether or not a new treatment plan should be developed. Plan validity is largely based on dose volume parameters within certain structures. If a relationship between relevant dose volume parameters and geometric changes is established, treatment plans could provide an estimate for the range of plan validity.

The dose distribution can be considered as a volume surrounding the target. When the catheters are displaced, this dose volume should move in an identical fashion. Ideally the dose is higher within the prostate, and decrease outwards as it reaches healthy tissues. Assuming this is the case, when the catheters move the average dose within the prostate will decrease. When this shift is along the longitudinal axis, it seems reasonable to expect two extremes where the dose distribution becomes invalid. Holding all other variables constant, this could provide the range in acceptable catheter displacements.

Changes in prostate volume are relatively easy to model, but determining the change in dose distribution associated with this volume change is complex. As the prostate changes shape, so do the catheters within the prostate, which alters the dose distribution relative to the catheters. Currently the only method for determining the difference in dose distribution between volume changes is to recalculate the dose distribution. This is a computationally intensive process, especially for considering a wide range of volume changes. Perhaps a model that predicts the dose distribution

variation as a function of volume deformation could be determined. This type of relationship would require more than one treatment plan, so it goes beyond the scope of this paper.

## 1.4 Objective

The goal for this project is to determine the maximum variations in geometry for a single plan. Average catheter shifts are expected to affect the dose volume parameters more than typical volume deformations [4]. By using MATLAB to model implant deformations, the affects catheter displacement and volume changes have on the dose distribution can be examined independently. The uncertainty in implant deformations should also be smaller than in clinical studies, because the position measurement are not limited by the spacing between CT scans. This reduction in uncertainty will provide a more concrete understanding of how dose distribution varies following an implant deformations.

# Chapter 2

# Theory

The dose distribution will be calculated using the two dimensional line source formalism recommended by AAPM [15]. In practice the source is cylindrical with a given radius and length $L$, but in this formalism the source will be assumed to be contained within a line of length $L$. Like the treatment itself, the model is highly sensitive to the source geometry relative to the point of interest, $P(r, \theta)$. Figure 2.1 contains the relevant geometric variables and constants.

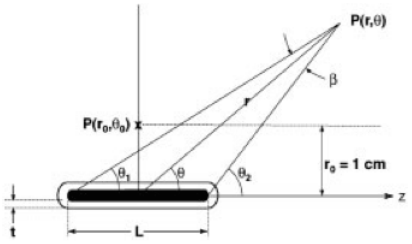


**Figure 2.1:** Coordinate system used for line source 2D formalism [15]

To calculate $\theta$, the dot product was utilized between a vector along the hypothetical line source, $\vec{V}_{LS}$, and the vector to the point of interest, $\vec{V}_{POI}$. $\vec{V}_{LS}$ was calculated as

$$\vec{V}_{LS} = P_i(x, y, z) - P_{i+1}(x, y, z) \tag{2.1}$$

Where $P_i(x, y, z)$ is the current dwell position and $P_{i+1}(x, y, z)$ is the next dwell position along the catheter. If there is no following dwell position then the vector

from the previous position will be used instead. Similarly $\vec{V}_{POI}$ is found as

$$\vec{V}_{POI} = P_i(x, y, z) - P(x, y, z) \tag{2.2}$$

And finally $\theta$ is found as

$$\theta = \arccos \frac{V_{LS} \cdot \vec{V}_{POI}}{|\vec{V}_{LS}||\vec{V}_{POI}|} \tag{2.3}$$

The main uncertainty with this angle traces back to the vector along the hypothetical line source, which is calculated assuming that the catheter is entirely straight. In practice catheters can bend so this issue may need to be addressed in the future if the catheter experiences bending much larger than 10° between dwell positions.

Air-kerma strength, $S_K$, is a source dependent constant. It represents the kinetic energy released in air after a photon has propagated one centimetre away from its source, following a trajectory along the perpendicular bisector.

The dose rate constant in water, $\Lambda$, is a constant defined by

$$\Lambda = \frac{\dot{D}(r_o, \theta_o)}{S_K} \tag{2.4}$$

Where $\dot{D}(r_0, \theta_0)$ represents the dose rate at the reference position, when the dose propagates through water.

The geometry function, $G_L(r, \theta_0)$, provides an effective inverse square correction based on the distribution of radioactivity within the source. As recommended by AAPM, the line source model will be used, as opposed to the point source model. The line source model accounts for the angle subtended by the line source tips, $\beta$, to $P(r, \theta)$

$$G_L(r, \theta) = \begin{cases} \frac{\beta}{Lr \sin\theta} & \text{if } \theta \neq 0 \\ (r^2 - \frac{L^2}{4})^{-1} & \text{if } \theta = 0 \end{cases} \tag{2.5}$$

Dose attenuation and scattering is accounted for by the radial dose function, $g_L$

$$g_L(r) = \frac{\dot{D}(r, \theta_0)}{\dot{D}(r_0, \theta_0)} \frac{G_L(r_0, \theta_0)}{G_L(r, \theta_0)} \tag{2.6}$$

As is common practice, a fifth order polynomial will be utilized in place of Equation 2.6 [15]. The coefficients for this polynomial are provided by the source manufacturer.

The final quantity of interest is the two dimensional anisotropy function $F(r, \theta)$, which represents the variation in dose delivery around the source. $F(r, \theta)$ is determined by interpolating the two dimensional anisotropy table provided by the source manufacturer. In this case $F(r, \theta)$ was tabulated at increments of 0.1mm for $r$ and $0.01^\circ$ for $\theta$. The table was interpolated using the *interp*2 function in MATLAB. Smaller increments for either $r$ or $\theta$ forced MATLAB to stop responding. Regardless, the increments selected produced results within 0.001% to when the two dimensional anisotropy table was interpolated separately for each point. This small approximation reduced computing time by over three orders of magnitude.

Now the two dimensional dose rate $\dot{D}(r, \theta)$ can be constructed as

$$\dot{D}(r, \theta) = S_K \cdot \Lambda \cdot \frac{G_L(r, \theta)}{G_L(r_0 \theta_0)} \cdot g_L(r) \cdot F(r, \theta) \tag{2.7}$$

Equation 2.7 will calculate the rate for dose delivery to a specified point.

# Chapter 3

# Methods

## 3.1 Treatment Plan

9.50 Gy was prescribed to treat a wax phantom with simulated prostate cancer. The phantom had structures representing the prostate, rectum, and urethra. A treatment plan using an $Ir^{192}$ source was generated on an Oncentra treatment planning system, which used IPSA to optimize the dose distribution.

Geometry in this treatment plan was manipulated using MATLAB. During manipulations, all parameters pertaining to the original treatment plan were taken to be exact values. In addition, all positions and relative distances were taken to be exact.

## 3.2 Developing Accurate Dose Calculations

To begin with, a method to calculate the dose at an individual point was determined. There were 21 control points in the treatment plan which provided a benchmark for the calculated dose (Figure 3.1). The standard deviation between the benchmarks and the calculated values was determined to be $\pm$ 0.12%. Uncertainty in the calculated dose was derived from the standard deviation from benchmark values, as determined by the commercial planning system.

## 3.3 Determining Structures

The structures within a treatment plan are outlined by contours. A uniform distribution of points within each contour was taken and saved as a collection corresponding

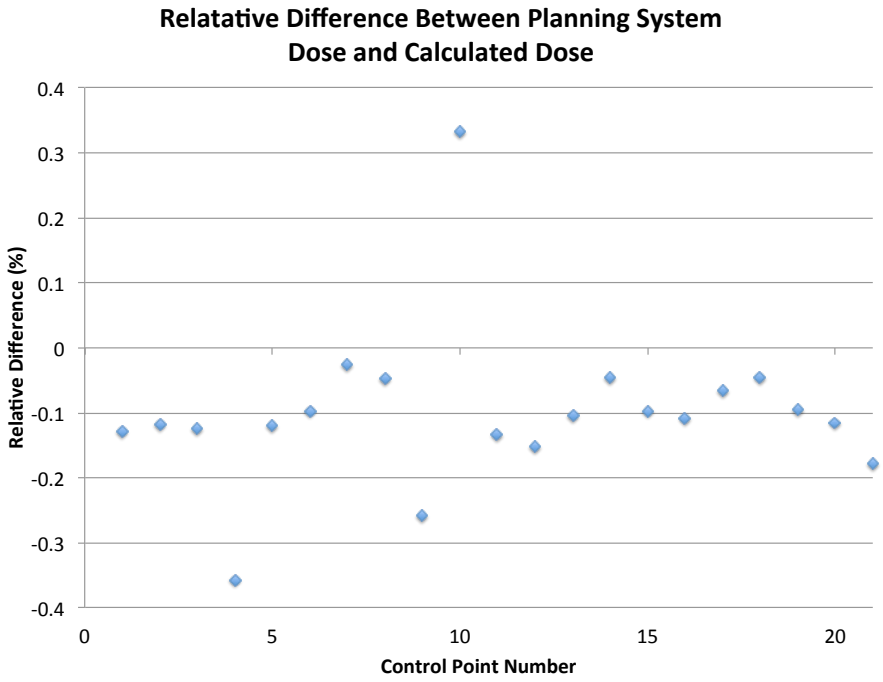


**Figure 3.1:** The relative difference between the dose to a point as determined by a commercial treatment planning system, in comparison to the dose calculated. These results reflect that the calculated dose will typically be an over estimate.

to their respective structures. For consistency purposes, the number of points representing each structure was within 1% of the commercial planning system.

After each structure represented by a collection of points, the dose at each point was calculated. From the collection of doses within each structure, the dose volume parameters were calculated as the fraction of points receiving the minimum dose associated with the dose volume parameter of interest. Plan validity was determined by cross referencing the dose volume parameters to the minimum safety standards put forth by ABS [2].

Several dose volume parameters pertaining to the prostate were supplied with the treatment plan. The standard deviation between calculated dose volume parameters and their accepted values was calculated as 0.3% (3.1). This standard deviation was taken to be the error in all calculated dose volume parameters.

| | Calculated | Commercial Planning System | Difference |
|---|---|---|---|
| $V_{100}$ | 94.41% | 94.19% | 0.22% |
| $V_{75.58}$ | 100.00% | 100.00% | 0% |
| $V_{150}$ | 25.29% | 24.91% | 0.38% |
| $V_{200}$ | 9.26 % | 9.67% | -0.41% |
| $V_{90}$ | 98.53% | 98.26 % | 0.27% |
| $V_{106.33}$ | 90.08 % | 90.00 % | 0.08% |

**Table 3.1:** Comparison of the dose volume parameters from calculations and the accepted values. The standard error in the difference is 0.3%.

## 3.4 Catheter Displacement

With a system in place to determine the dose volume parameters, the resilience of the treatment plan to geometric changes was tested. A unit vector parallel to the average catheter was determined to represent the longitudinal axis. Catheter shifts were limited to the longitudinal axis, where a negative or positive shift represented a shift in the inferior or superior directions respectively. Catheter movement was simulated by shifting the dwell positions in 0.1 mm increments. The dose volume parameters were calculated at each increment. When these increments brought the plan to the brink of failing, the increments were reduced to determine the first point where the plan fails.

## 3.5 Prostate Volume Change

Prostate volume changes were taken to occur isotropically [6]. To simulate volume changes, a temporary coordinate system was established that centred the prostate on the origin. Any points associated with structures within the prostate were shifted into the same coordinate system. All the points contained within the prostate volume were multiplied by the cubic root of the desired fractional volume change. The cubic root of the volume change was incremented at 0.1% intervals. Similar to the catheter shift scenarios, the dose volume parameters were calculated following each increment.

Catheters and the urethra and within the prostate; both of these structures are relatively flexible. As such, it is reasonable to model any points representing these structures within the prostate, as being shifted in the same manner coinciding with the prostate volume change.

# Chapter 4

# Results

$V_{100}$, $U_{125}$ and $DHI$ were recorded for catheter displacements along the longitudinal axis and prostate volume deformations. For this particular plan the dose delivered to the rectum as it related to the minimum ABS guidelines was negligible, so it is not included in this analysis.

## 4.1 Catheter Displacement

Dose volume parameters important to plan validity were determined as the catheters were shifted in the superior and inferior directions (Figure 4.1). In both scenarios the plan failed when $V_{100} < 90\%$, which occurred once the catheters were shifted either $4.15 \pm 0.15$ mm in the superior direction or $3.70 \pm 0.15$ mm in the inferior direction. Both $U_{125}$ and $DHI$ were within tolerance levels during catheter displacement, and showed no indications of compromising the treatment plan after the catheters were displaced 7.5 mm.

## 4.2 Prostate Volume Changes

The prostate was expanded by 34% and compressed by 27%, relative to its original volume. During these volume deformations the dose volume parameters were determined at regular intervals (Figure 4.2). In the expanding prostate case $V_{100}$ was the first parameter to make the plan invalid. The plan failed when the volume was increased by $10.7 \pm 0.5\%$ of the original volume. When the prostate was compressed, $U_{125}$ was the first parameter to fail. The failure occurred once the prostate was compressed by $11.0 \pm 0.2\%$ from its original volume.

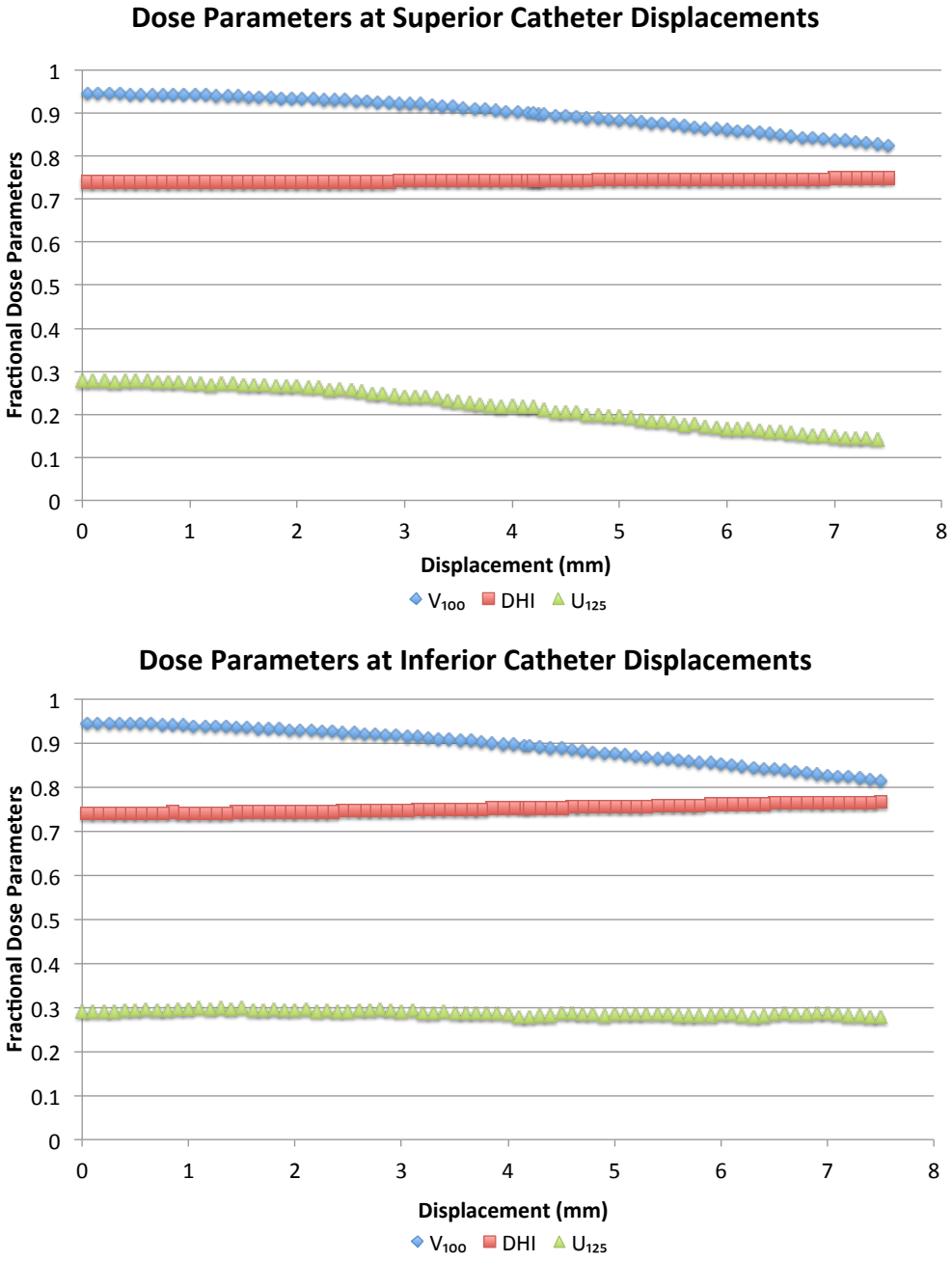


**Figure 4.1:** Dose volume parameters plotted against catheter displacement in both the superior and inferior directions.

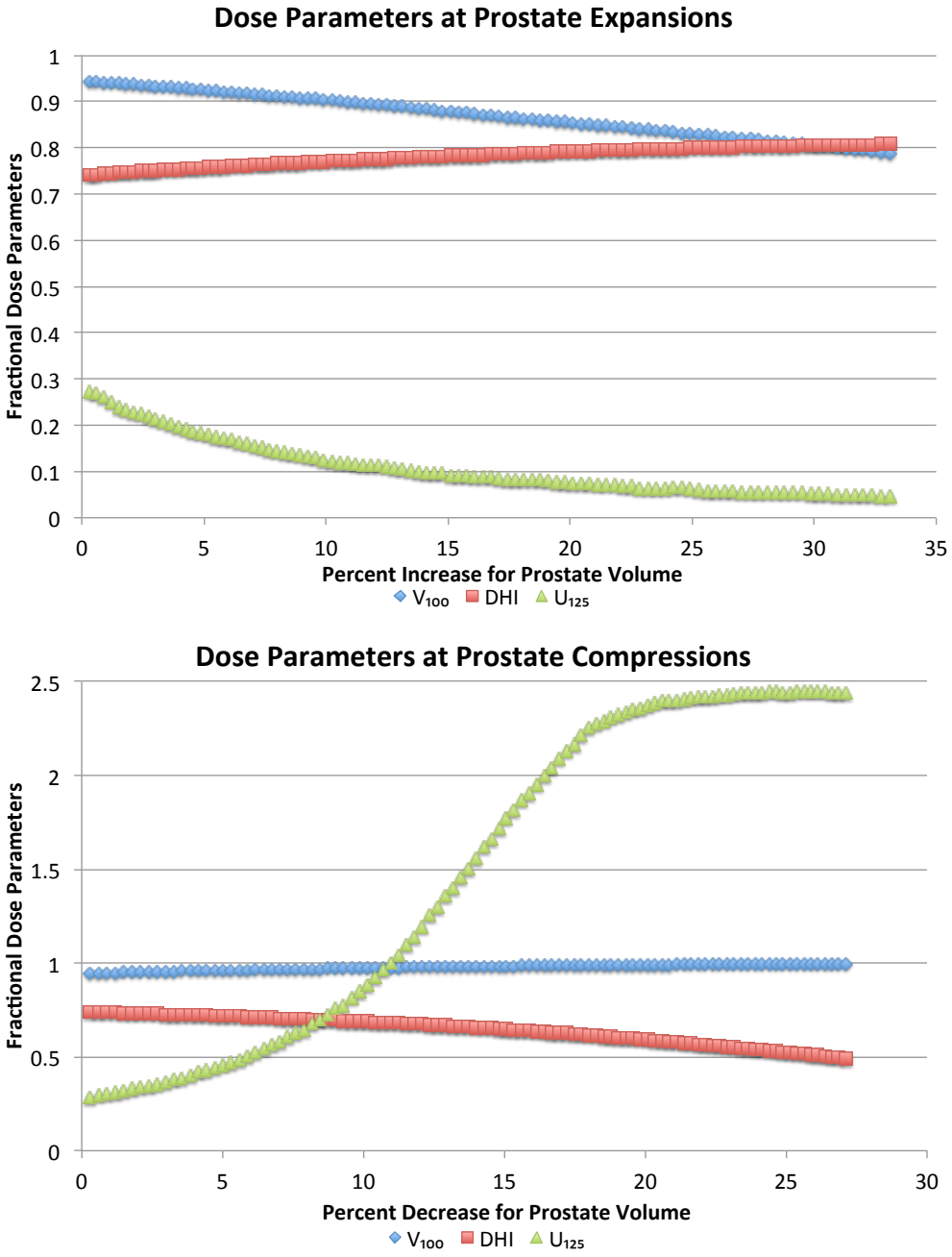


**Figure 4.2:** Dose volume parameters were recorded at regular intervals as the prostate was expanded and compressed.

# Chapter 5

# Discussion

The maximum catheter shifts associated with a valid treatment plan were determined to be 3.70 ±0.15 mm and 4.15 ±0.15 mm, for inferior and superior displacements respectively. These results are within the 3mm to 6mm range found in clinical settings to be valid for 75% of treatments [10]. From clinical trials, it is reasonable to expect the catheters to shift between the first and second fraction by 7.6 mm. From Figure 4.1, it can be inferred that the this specific treatment plan would no longer be valid after an average catheter displacement. However following the second fraction, catheter displacement is typically bellow 3 mm. This suggests, that later in the treatment, knowing the range in acceptable catheter displacements could pose as a more valuable asset than it would in the early stages.

The allowed volume deformations were determined to be a 10.7 ± 0.5% increase and an 11.0 ± 0.2% decrease from the original prostate volume. These volume changes were significantly greater than the average volume deformations determined in clinical trials. Prostate volume is expected to deviate between 1% and 2.7% from the original volume over the course of an entire treatment. Figure 4.2 demonstrates that the plan would still be valid after undergoing an average change in prostate volume.

After comparing the plan validity to average geometric changes, catheter displacement was observed to be a larger factor than volume fluctuations, in dose distribution variation. These comparisons are in agreement to clinical trials which deem catheter displacement as the primary source for dose distribution variation [4].

The uncertainty in catheter displacement for clinical trials in limited by the spacing of CT scans [9]. In contrast, using techniques in MATLAB, the catheter positions can be known to absolute precision. With this type of precision, the limits of geometric variation can be accurately determined. So as where clinical trials were citing

uncertainties in catheter position at $\pm$ 1 mm, the techniques applied using MATLAB produced uncertainties of $\pm$ 0.15 mm. Additionally, by using MATLAB the relationship between the evolution of an implant deformation and dose distribution variation, can be studied to a closer degree. For example, from Figure 4.2, $U_{125}$ increases rapidly in the compression range between 10% and 18%. This behaviour would be difficult to observe in a clinical setting, because patient well being must be considered so CT scans can only be taken so often.

The $DHI$ before implementing geometric changes was $0.740 \pm 0.003$, which did not satisfy the standards set by ABS for breast cancer ($DHI \geq 0.750$). Since the treatment plan was generated by a commercial planning system, it is reasonable to assume that the $DHI$ guidelines for breast cancer do not translate well for prostate cancer. When treating the prostate with HDR-BT, catheters must be inserted within the prostate but away from the urethra, which runs through the prostate; breast cancer treatment does not have a comparable issue. This difference in catheter placement freedom may explain the difference between the acceptable $DHI$ values for the two treatments. As a result, the minimum acceptable $DHI$ value was taken to be $0.62 \pm 0.06$, as found through research independent from ABS [14]. Compressing the prostate was the only scenario to pose a negative affect on $DHI$. When the prostate was compressed by 17.8% $\pm$ 0.2% the $DHI$ dropped bellow an acceptable threshold.

From this treatment plan $V_{100} \geq 90\%$ is the factor that limits plan validity in cases of catheter displacement and prostate expansion. Under the same scenarios, $U_{125}$ and $DHI$ improved or remained relatively constant. In contrast, during prostate compression $U_{125}$ and $DHI$ became less ideal as $V_{100}$ tended towards 100%. These tendencies may be unique to this treatment plan. Employing these techniques against several different treatment plans, devised for multiple patients, could verify the universality of these tendencies.

# Chapter 6

# Conclusion

Using the dose calculation method developed by AAPM, the dose distribution for a supplied treatment plan was determined. The plan was then subject to variations in anatomical geometry, relevant to treating prostate cancer with HDR-BT. Extreme variations in geometry were determined once the plan failed in accordance with ABS guidelines. The results were in good agreement to clinical trials with sample sizes larger than fifty patients.

Future work should be directed towards applying the techniques utilized in this project towards historical treatment plans. This would provide a better understanding as to how a treatment plan changes over the course of HDR-BT. If implemented in a planning system the geometric tolerances of a treatment plan could help to assist an oncologist in selecting a treatment plan, especially in the later stages of treatment.

# Bibliography


[1] Canadian Cancer Society, "Canadian cancer statistics - special topic cancer," 2014.

[2] I.-C. Hsu *et al.*, "American brachytherapy society prostate high-dose rate task group," 2008.

[3] D. R. Hill, "High dose rate brachytherapy method."

[4] E. Mullokandov *et al.*, "Analysis of serial ct scans to assess template and catheter movement in prostate hdr brachytherapy brachytherapy," *Elsevier*, vol. 58, no. 4, pp. 1063–1071, 2004.

[5] P. J. Hoskin *et al.*, "High dose rate afterloading brachytherapy for prostate cancer: catheter and gland movement between fractions," *Radiotherapy and Oncology*, vol. 68, pp. 285–288, 2003.

[6] Y. Kim, I.-C. Hsu, E. Lessard, J. Vujic, and J. Pouliot, "Dosimetric impact of prostate volume change between ct-based hdr brachytherapy fractions," *Int J Radiat Oncol Biol Phys*, vol. 59, pp. 1208–16, Jul 2004.

[7] S. J. Damore, A. M. Syed, A. A. Puthawala, and A. Sharma, "Needle displacement during hdr brachytherapy in the treatment of prostate cancer," *Int J Radiat Oncol Biol Phys*, vol. 46, pp. 1205–11, Mar 2000.

[8] T. Takenaka, K. Yoshida, M. Ueda, H. Yamazaki, S. Miyake, E. Tanaka, M. Yoshida, Y. Yoshimura, T. Oka, and K. Honda, "Assessment of daily needle applicator displacement during high-dose-rate interstitial brachytherapy for prostate cancer using daily ct examinations," *J Radiat Res*, vol. 53, no. 3, pp. 469–74, 2012.

[9] S. Kawakami, H. Ishiyama, T. Terazaki, I. Soda, T. Satoh, M. Kitano, S. Kurosaka, A. Sekiguchi, S. Komori, M. Iwamura, and K. Hayakawa, "Catheter

displacement prior to the delivery of high-dose-rate brachytherapy in the treatment of prostate cancer patients," *J Contemp Brachytherapy*, vol. 6, pp. 161–6, Jun 2014.

[10] T. A and other, "A small tolerance for catheter displacement in high-dose rate prostate brachytherapy is necessary and feasible.," *Int J Radiat Oncol Biol Phys*, pp. 1066–1072, 2010.

[11] I.-C. J. Hsu, E. Lessard, V. Weinberg, and J. Pouliot, "Comparison of inverse planning simulated annealing and geometrical optimization for prostate high-dose-rate brachytherapy," *Brachytherapy*, vol. 3, no. 3, pp. 147–52, 2004.

[12] D. Jacob, A. Raben, A. Sarkar, J. Grimm, and L. Simpson, "Anatomy-based inverse planning simulated annealing optimization in high-dose-rate prostate brachytherapy: significant dosimetric advantage over other optimization techniques," *Int J Radiat Oncol Biol Phys*, vol. 72, pp. 820–7, Nov 2008.

[13] M. Keisch *et al.*, "American brachytherapy society breast brachytherapy task group," 2007.

[14] I. Sumida, H. Shiomi, Y. Yoshioka, T. Inoue, E. Lessard, I.-C. J. Hsu, and J. Pouliot, "Optimization of dose distribution for hdr brachytherapy of the prostate using attraction-repulsion model," *Int J Radiat Oncol Biol Phys*, vol. 64, pp. 643–9, Feb 2006.

[15] M. J. Rivard, B. M. Coursey, L. A. DeWerd, W. F. Hanson, M. S. Huq, G. S. Ibbott, M. G. Mitch, R. Nath, and J. F. Williamson, "Update of aapm task group no. 43 report: A revised aapm protocol for brachytherapy dose calculations," *Med Phys*, vol. 31, pp. 633–74, Mar 2004.